Int. J. Heat Mass Transfer. Vol. 19, pp. 839–848. Pergamon Press 1976. Printed in Great Britain

LAYERED THERMOHALINE NATURAL CONVECTION

T. R. MANCINI, R. I. LOEHRKE and R. D. HABERSTROH
Colorado State University, Fort Collins, CO 80523, U.S.A.

(*Received* 30 *October* 1975)

Abstract—The results of two quasi-steady experiments in layered, double-diffusive convection are presented and interpreted in terms of a steady-state model. In the experiments heat and salt are transported upward through two horizontal convecting layers of water which are separated by a thermocline, a region of large temperature and concentration gradients. As the thermocline stability number $\beta_c\Delta C/\beta_t\Delta T$ increases, the thermocline becomes thicker and the fluxes of heat and salt decrease. These two characteristics of the thermohaline system are shown to be consistent with a conduction–convection model which views the thermocline as a conduction region separating two convective boundary layers. That molecular diffusion is the dominating transport process in the central portion of the thermocline is experimentally verified. The thickness of the conducting region is found to vary with the imposed boundary conditions in such a manner as to maintain conditions of near neutral stability across the boundary layers.

NOMENCLATURE

C,	salt concentration per unit volume;
C_p,	specific heat capacity at constant pressure;
D,	diffusivity;
F_c,	salt flux;
F_H,	heat flux;
h,	convective transport coefficient;
K,	thermal conductivity;
l,	depth of a convecting layer;
L,	diffusion thickness of a thermocline;
L',	intercept thickness of a thermocline based on the density profile;
T,	temperature;
z,	vertical position referred to the bottom of the test section.

Greek symbols

β_c,	coefficient of fractional density change due to a unit change in concentration;
β_t,	coefficient of fractional density change due to a unit change in temperature;
ρ,	density.

Dimensionless parameters

Le,	Lewis number, $\dfrac{D_t}{D_c}$;
Nu_l,	Nusselt number, $\dfrac{\text{actual heat flux}}{\text{conduction heat flux}} = \dfrac{F_H l}{K\Delta T_l}$;
Sh_l,	Sherwood number, $\dfrac{\text{actual mass flux}}{\text{diffusion mass flux}} = \dfrac{F_c l}{D_c \Delta C_l}$;
Sy,	stability number, $\dfrac{\beta_c\Delta C}{\beta_t\Delta T}$.

Subscripts

c,	refers to concentration properties;
l,	refers to a convective boundary layer;
L,	refers to the diffusive region of the thermocline;
t,	refers to thermal properties;
T,	refers to bulk-to-bulk parameters across the thermocline.

INTRODUCTION

BUOYANCY driven convection which depends on the diffusion of two quantities with different molecular diffusivities has been the subject of increasing attention in recent years. Much of the past work and many of the applications are reviewed by Turner [1, 2]. Two features of double-diffusive convection in horizontal fluid layers which set it apart from ordinary natural convection are that convection can take place even though the density decreases in the upward direction and that the convecting system is often layered (composed of two or more well-mixed regions separated by interfaces across which are large gradients in the concentration of the diffusing species). This paper deals with an experimental study of thermohaline convection in which heat and salt are transported upward through horizontal layers in a tank of water. In the experiments described the overall stability number Sy of the system is greater than one; that is, the density of the fluid at the bottom of the tank is greater than at the top.

The experiments of Turner [3] and Shirtcliffe [4] are closely related to the present investigation. They are similar to each other in that both are two-layer, transient experiments. Turner added heat to the bottom of a tank which contained two layers of stably stratified water with different salinities, separated by a sharp interface. He measured the changes of temperature and concentration in the two layers with time and from these changes inferred the heat and salt fluxes through the interface. The stability number of this interface decreased with time as the salt concentrations in the two convecting layers equalized. In Shirtcliffe's experiment a layer of salt water was floated above a layer of sugar water. He observed that the interface between the two layers thickened with time as the stability number across the interface increased. From measured concentration profiles through the interface he concluded that the gradients were large enough to account for the fluxes by molecular diffusion alone.

In both experiments the flux ratio

$$\frac{\beta_c F_c}{\beta_t F_H/\rho C_p}$$

was correlated with the thermocline stability number. Turner found that this ratio decreased with increasing stability number at low stability number but remained constant at a value of 0.15 for $Sy_T > 2$ in his heat–salt system. Linden [5] has estimated that the region of variable flux ratio in Turner's experiments corresponds to the region where turbulent entrainment across the interface is important.

In Shirtcliffe's sugar–salt experiment a constant value of 0.6 was observed for this flux ratio over the range $1.1 < Sy_T < 3$ where F_H and F_c corresponded to the fluxes of salt and sugar respectively. Shirtcliffe attributes the difference between his measured values and Turner's to a Lewis-number dependence but no satisfactory explanation has been offered for the constancy of the flux ratio over a wide range of stability numbers nor for the thickening of the interface.

Huppert [6] analyzed a series of interfaces and found constancy of the flux ratio to be a necessary condition for stability. He also found, from an analysis of Turner's single-interface data, that the other required condition for stability, the form of the variation of heat flux through the interface with stability number, was satisfied. This observation led him to conclude that a multi-layered system would be stable provided the individual interfacial stability numbers were greater than two.

One of the original objectives of the present experimental program was to study the stability of a multi-layered system and the turbulent transport through the entrapped convecting regions. Early results of this study [7], particularly at high interface stability numbers, indicated the need for further study of a two-layer system under steady or nearly steady boundary conditions.

In this paper the results of several layered heat–salt experiments are described. The first experiment was performed in an apparatus in which both heat and salt could be added to the bottom of a tank of salt water and removed from the top. In the second set of experiments, a smaller, closed test section was used. Heat was continuously added to the bottom and removed from the top, but the upper and lower boundaries were impermeable to salt.

PERMEABLE BOUNDARY EXPERIMENT

The experimental apparatus for the main experiment consists of a test-section and two conditioner systems which supply hot, salty water at the bottom of the test section and cool, fresh water at the top [7]. The test section is an open-ended box formed by four square walls 0.67 m on each side. The walls are constructed of Plexiglass 1.25-cm thick and insulated on the outside by 7.5 cm of styrofoam. Pellon (a polyester felt) sheets 0.13 cm thick separate the test section at the top and bottom from the two conditioning systems. The water in the upper conditioning system is degassed to remove the air and cooled before passing over the membrane at the top of the test section. A manifold distributes the flow evenly among 10 channels 5 cm wide, 2.5 cm high and 0.67 m long, located directly above the upper membrane. The water in adjacent channels flows in opposing directions at low velocity. A second manifold at the downstream end of the channels collects the water which is then discarded to drain. The temperature rise of the water between the inlet and outlet manifolds is negligible and the concentration difference is also quite small (several hundred ppm). The hot, salty water in the lower conditioning system is recirculated beneath the lower membrane in a similar manner. Its temperature is maintained by heaters located in the storage tank which is part of the lower loop as well as by heaters located beneath the bottom of the test section. Granulated salt may be added to the storage tank to maintain the concentration in the lower loop. This salt dissolves before the water reaches the bottom of the test section. The counterflow arrangement and the Pellon membranes minimize the momentum transfer from the conditioner flows to the salt water in the test section. No circulations resulting from these supply systems were observed in the test section.

A thermocouple-conductivity probe is used to obtain temperature and concentration profiles through the convecting fluid layers and intervening interface. In Fig. 1 the "L"-shaped probe and its shadow are pictured directly above the top of the interfacial or thermocline region separating two convecting layers of salt water. The thermocouple is constructed from 0.13 mm copper and constantan wires which form a bead 0.2 mm in diameter. The thermocouple is referenced to an ice bath at 0°C, and its output is amplified using a Keithley microvoltmeter. The conductivity cell is a 0.7-cm dia ring-and-tip configuration constructed from 0.13 mm platinum wire through which a 10 kHz AC current is passed [8, 9]. The ring and tip of the conductivity cell are platinized. The thermocouple bead and the tip of the conductivity cell are separated by 0.5 cm in the same horizontal plane. An RMS voltmeter is connected in parallel with the conductivity cell; its output is inversely proportional to the electrical conductivity of the saline solution at the probe tip. Because the probe cannot be removed from the test section during the course of the experiment, the cell constants tends to drift and it is necessary to calibrate the conductivity cell for each data run. This is done by removing salt water samples from the well-mixed regions of the test section and measuring the concentrations with a Beckmann bridge and calibrated dip cell. Both the thermocouple and conductivity cell outputs are recorded on two channels of a Hewlett–Packard x–y plotter. The x-axis input to the plotter is the output of a voltage divider which is mechanically

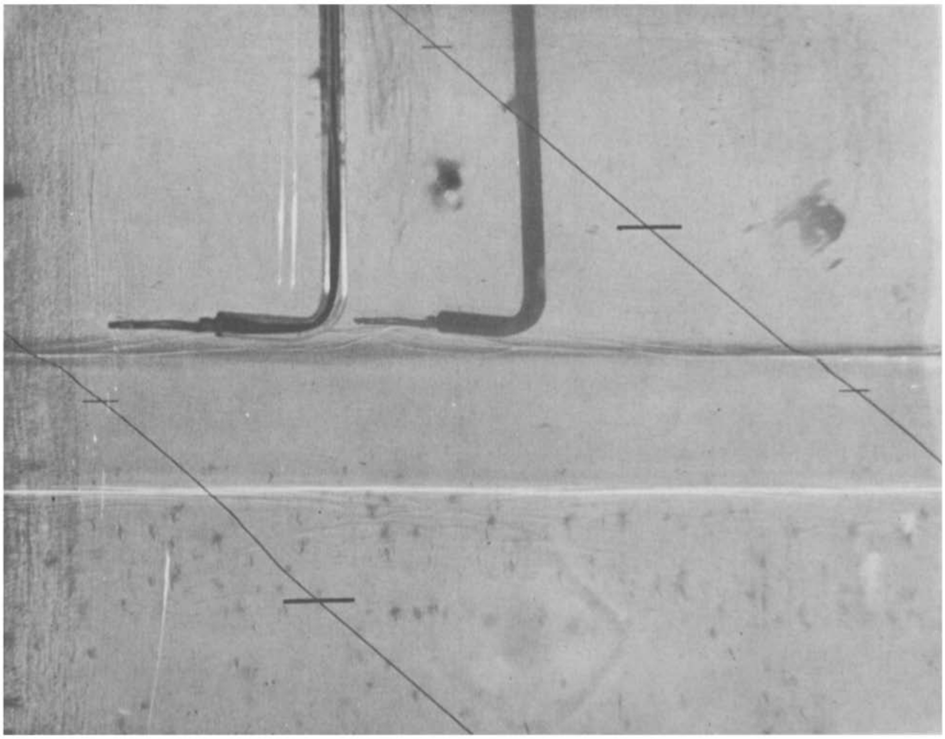

FIG. 1. Shadowgraph picture of a thermocline. The thermocouple-conductivity probe and its shadow are shown immediately above the top of a thermocline (indicated by the dark horizontal line). The horizontal white line is the bottom of the thermocline.

coupled to the probe shaft thereby indicating the vertical position of the probe tip within the test section. The traverse assembly is mounted above and at the center of the test section.

The maximum uncertainty in the temperature measurement is ±0.17°C as limited by the amplifier. The salt concentrations can be measured to within a ±4 parts per thousand (ppt) at high concentrations and ±2 ppt at lower concentrations. The thermocouple conductivity probe can be positioned within 0.7 mm with good repeatability.

To begin the experiments the lower half of the test section was filled with salt water and the upper half with fresh water to form a sharp interface midway up the tank. Hot salt water was supplied at the bottom of the test section and cool, fresh water at the top. As the experiment progressed a lower convecting layer (layer *A*) and an upper convecting layer (layer *B*) were formed separated by an interfacial region of large temperature and salt gradients (the thermocline). The test section was traversed with the thermocouple-conductivity probe once each day during the 65-day test period. Completion of a typical traverse could require as much as 1.5 h depending on the thickness of the thermocline. During a traverse the probe was stepped through the test section at increments of from 1.5 to 3 mm. The size of these steps was determined by the location of the probe tip and the thickness of the thermocline, the smaller increment being used when the thermocline was thin or the gradients large. The probe was allowed to remain at each location until the transients had subsided (approximately 1 min), then the signals from the thermocouple and the conductivity cell were recorded for a period of 30 s. The average values over the sample period for temperature and concentration at each location were later determined and used in plotting the vertical profiles. After the traverse was completed, salt water samples were removed from the two convecting layers in order to calibrate the conductivity cell. Conductivity readings were then corrected for temperature and converted to concentrations with Office of Saline Water property data. Typical temperature, concentration and density profiles (for the 21st day of the experiment) are shown in Fig. 2. Density changes are chiefly dependent on large changes in concentration. The small, destabilizing effect of the temperature profile at the top of the thermocline is not perceptible on this density scale.

The bulk temperature and concentration histories for this experiment are shown in Fig. 3. The experiment was quasi-steady in that salt lost from the lower convecting layer was not, for the most part, replenished. Heat, however, was continuously added and removed from the test section and salt was continuously removed at the upper boundary. Some perturbations to the boundary conditions were provided through the addition of salt to the lower conditioner system three times during the experiment and by changes in the power supplied to the lower system twice over the 65-day test period. Unscheduled changes in the boundary conditions were unavoidable because of the duration of the experiment. These uncontrolled influences were of two types, first, power outages which resulted in loss of circulating water flow and heat input, and, second,

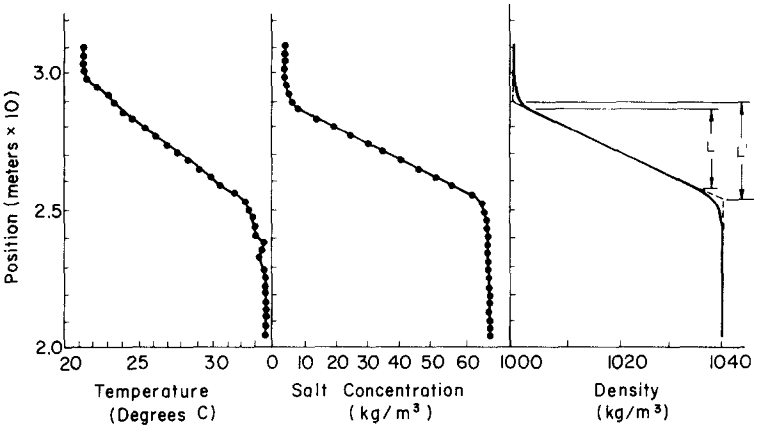

FIG. 2. Temperature, concentration and density profiles on the 21st day of the experiment. The linear diffusion thickness L, and the intercept depth of the thermocline L', are shown on the density profile.

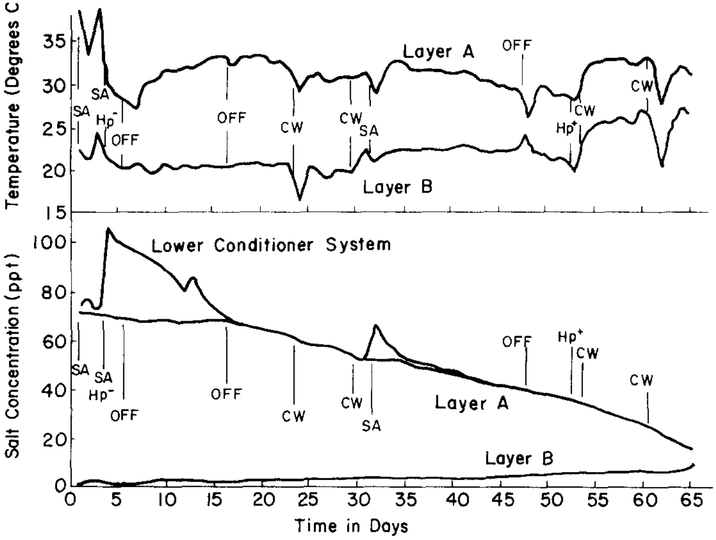

FIG. 3. Temperature and concentration histories of the convecting layers for the permeable boundary experiment. SA is a salt addition to the lower conditioner system. HP± refers to an increase or decrease in the power supplied to the heaters. CW is a drop in the cooling water temperature and "off" is a power outage.

losses of hot water supply to the constant temperature mixing valve which supplied the upper conditioner system resulting in a drop in the temperature of the upper cooling water. The duration of these excursions ranged between three and twelve hours. When the power was lost the system would tend toward thermal equilibrium; due to the low mass diffusivity, however, very little effect could be seen in the concentrations. A change in the temperature of the fresh water conditioning system resulted in a readjustment of the temperature level in the test section.

The changes in the temperature level on the 23rd and 61st days were due to a change in the cooling water temperature. The equilibration of the two temperatures on the 46th day is the result of a power outage. Following the salt addition on the third day, the concentration difference between the lower system and convecting layer *A* increased. The Pellon membrane clearly inhibited convective mixing between these two regions. The concentration of the lower system reached a peak and then declined while the concentration in layer *A* remained steady. On the 16th day of the experiment the two concentrations, the lower system and layer *A*, equalized and continued to decrease gradually throughout the remainder of the experiment diverging briefly when salt was added on the 31st day. The interface between convecting layers thickened initially forming a large region over which the gradients of temperature and concentration were nearly constant. Then, in response to the slowly changing boundary conditions of temperature and concentration, the interface thinned slowly as the stability of the system decreased. The growth and thinning of the thermocline did not proceed at the same rates on the top and bottom of the interface. In the latter stages of the experiment the top was actually growing while the bottom was being eroded at a faster rate; the appearance was that of a thinning interface rising in the test section. This test was terminated when the thermocline rose above the range of travel of the temperature-conductivity probe. This "climbing thermocline" phenomenon was also observed in another apparatus with entirely different upper and lower boundary conditions and different side-wall heat-loss control. These experiments are described in the next section.

Several methods were used to assess the properties of the thermohaline system. Shadowgraph visualization was achieved by illuminating the test section with a small light source located about 4 m away from and on the same level as the thermocline. Variations in the intensity of light which has passed through the test section reveal regions where the second spatial derivative of density is non-zero. Figure 1 is a shadowgraph picture of a thermocline; the lower boundary is indicated by the white horizontal line and the upper boundary by the dark line. The "L"-shaped probe and its shadow are located just above the upper boundary layer. The diagonal lines are straight lines on a screen as viewed through the test section. Unsteady convective motions in the two boundary layers were clearly visible as moving, small-scale shadows some of which are visible in Fig. 1. The three-dimensional character of these motions was apparent when the light source was moved below or above the thermocline level. No motion could be detected in the central portion of the thermocline or in the two well-mixed regions. Dye injection into the system indicated the existence of strong mixing motions within the convecting layers and little or no motion at all within the thermocline. The dye would disperse in a matter of minutes when placed in a convecting layer. Upon injection into the thermocline, however, the dye remained almost stationary with only a very slow horizontal drift. A distinct coloration persisted in the thermocline for a period of days. In addition to the visualizations, temperature–time histories were taken at various positions within the thermocline and convecting layers; an example of such a history is shown in Fig. 4. Examination of Fig. 4 indicates that there is much activity within the boundary layers and very little in the thermocline region. While this was generally true for all thermoclines, the thinner ones did exhibit a low-frequency temperature oscillation which became more pronounced as the thermocline became thinner. In addition, the fluctuations within the boundary layers were observed to be more vigorous for thin thermoclines than for thicker ones.

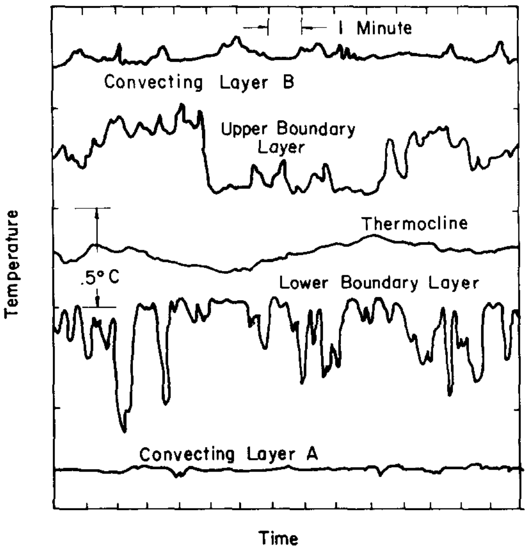

FIG. 4. Temperature vs time traces at several positions within a thin thermocline. These data were recorded sequentially. The mean temperatures are: convecting layer *A*, 29.7°C; lower boundary layer 29.1°C; thermocline 27.0°C; upper boundary layer 25.4°C; and convecting layer *B*, 25.3°C.

The visualizations, temperature–time histories at various positions, and the linear profiles of temperature and concentration within the thermocline indicate that molecular diffusion is the dominating transport process through the central region. A measure of the size of this central region was made by estimating the distance between the two points at which the smoothed mean density profiles first deviated from an extrapolation of the linear interior portion of the profile. The diffusion length *L* defined in this manner and illustrated in Fig. 2 is slightly smaller than the length *L*′ defined as the distance between the points of intersection of an extrapolation of the linear central portion of the profile to the bulk values of density in the convecting layers. *L*′ corresponded closely for thick thermoclines to the distance between the locations at the interior of the thermocline where the shorter period temperature fluctuations were first detected.

The size of the thermocline as characterized by *L* and *L*′ over the course of the experiment is shown in Fig. 5 along with a history of the stability of the system represented by the stability parameter

$$S_{YT} = \frac{\beta_c \Delta C_T}{\beta_t \Delta T_T}.$$

The thermocline thickness increased over the first 13 days of the experiment and decreased thereafter with but two exceptions. On the 33rd and 49th days the thermocline thickened as a result of salt addition and a system shut-down, respectively. The stability number shows the same general trend as the length. It dropped off quickly after the start-up perturbation, and peaked again on the 32nd and 48th days of the experiment.

The heat and salt fluxes for this experiment were calculated from the temperature and concentration gradients through the thermocline using the conduction equations

$$F_H = -K\frac{\mathrm{d}T}{\mathrm{d}z} \tag{1}$$

and

$$F_C = -D_c\frac{\mathrm{d}C}{\mathrm{d}z}. \tag{2}$$

K and D_c are the thermal conductivity and mass diffusivity, respectively, and $\mathrm{d}T/\mathrm{d}z$ and $\mathrm{d}C/\mathrm{d}z$ are the vertical temperature and concentration gradients at

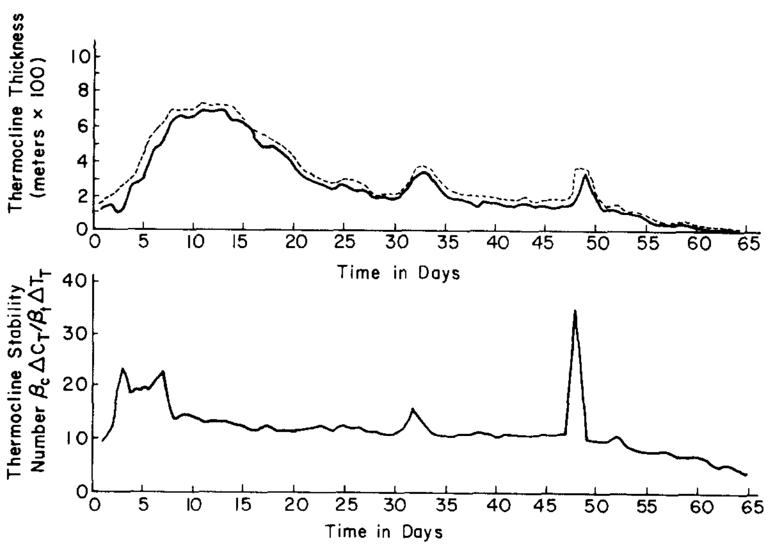

Fig. 5. Thermocline diffusion and intercept thicknesses, and stability number vs time.

the center of the thermocline as determined from profiles such as Fig. 2. The heat flux ranged from 50 to 300 W/m^2 and the salt flux ranged from 0.004 to 0.016 kg/m^2-h over the course of this experiment. A direct check of the applicability of equations (1) and (2) to the central region of the thermocline by independent measurements of the fluxes could not be made because of the open nature of the upper and lower test-section boundaries in this experiment. For this reason a second apparatus with closed upper and lower boundaries was constructed and a series of two layer experiments was performed. These experiments are described in the next section.

CLOSED TEST SECTION EXPERIMENTS

The test section of the apparatus for the secondary experiments is a 0.33 m, cubic tank with 0.64 cm Plexiglass sidewalls and a 0.64 cm brass bottom. The top plate conditioner system consists of 0.64 cm coiled copper tubing immersed in the water at the top of the test section. An aluminum sheet 0.5 mm thick is located directly beneath the cooling coils to isolate them from the water in the test section and to form a flat boundary at the top similar to the one at the bottom. Water from a constant-temperature mixing valve flows through the copper tubes providing a fixed-temperature boundary condition at the top. Two resistance heaters stacked one above the other are located below the 0.64 cm thick brass plate which forms the bottom of the test section; the lower heater acts as a guard heater to eliminate heat loss downward from the upper, main heater. Two methods were used to account for sidewall heat losses. During some of the experiments the test section was surrounded by 5 cm of styrofoam insulation. The sidewall losses were calibrated for effects of the temperature difference between the water in the test section and ambient air, and the depth of convecting layer *A*. The second configuration used sidewall guard heaters on the lower half of the test section to eliminate sidewall losses.

The instrumentation and procedures used in these experiments were identical to the ones used in the permeable-boundary experiments. The test section was initially layered with two concentrations of salt water with the interface positioned midway up the tank. No salt addition or removal occurred in these experiments. In contrast to the permeable-boundary experiments, a direct measurement of the power supplied to the primary, lower plate heater could be related to the upward flow of heat through the test section. This heat flow could then be compared with that calculated using the diffusion equation (1) and the temperature gradient in the thermocline.

The calibration curve for the test section sidewall heat losses has an uncertainty of ±1 W. Combined with the ±1.5% accuracy of the input power measurement, this suggests an overall uncertainty of ±1.45 W in the heat flow (at 30 W) as based on the power supplied to the primary heater.

Seven experiments were performed to test the hypothesis that the transport through the central portion of the thermocline is by molecular diffusion. In experiments 1–4 the test section was insulated with styrofoam only. Experiments 5–7 had guard heaters located around the lower half of the test section.

The temperature and concentration histories of the convecting layers and the thermocline position for experiment 6 are shown in Fig. 6. The cooling water temperature was lowered on days 8 and 11, and the heater power was increased on the 9th and 11th days of the experiment. The locations on the top and bottom of the thermocline were determined using the intercept method and the concentration profile, as in Fig. 2. As the stability number decreased during the course of the experiment the thermocline thinned and rose in the test section.

A comparison of the measured power input with the heat flow calculated from the temperature gradient through the thermocline is shown in Fig. 7 for all seven experiments. In the first four experiments the power

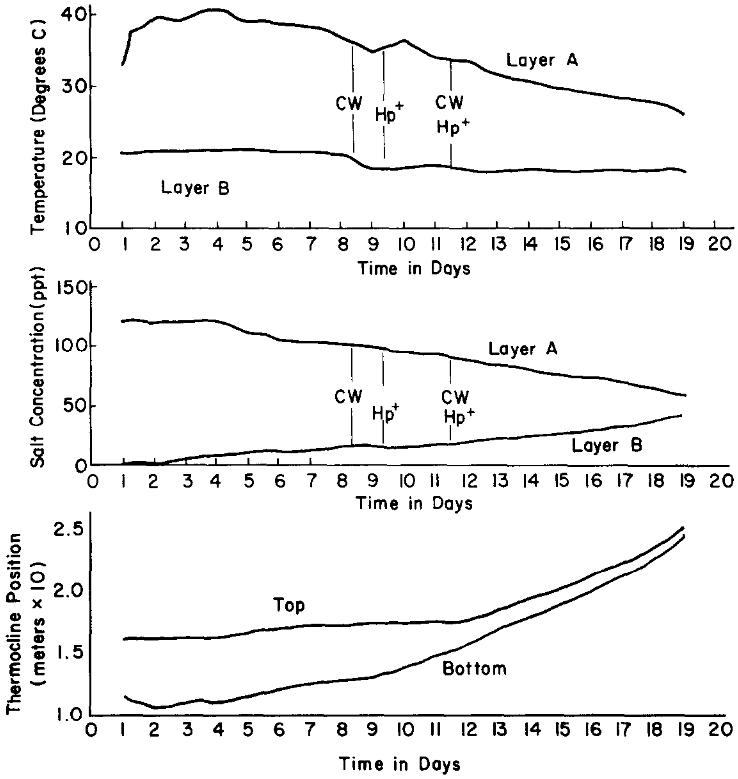

Fig. 6. Temperature and concentration histories and thermocline position for closed test section experiment 6.

supplied by the primary heater was corrected for sidewall heat losses and the change in energy with time of the lower convecting layer. For experiments 5–7 guard heaters were positioned on the lower half of the test section sidewalls. Even for these runs some sidewall corrections were required when unguarded areas were exposed by the rising thermocline. Transient data at start-up (during the first 2 or 3 days) and after changes in the cooling water temperature and power level were neglected. The largest discrepancies between the measured heat flow and the gradient estimates are associated with high fluxes through thin thermoclines. Under these conditions the uncertainty in the temperature gradient estimates is large enough to account for much of the difference.

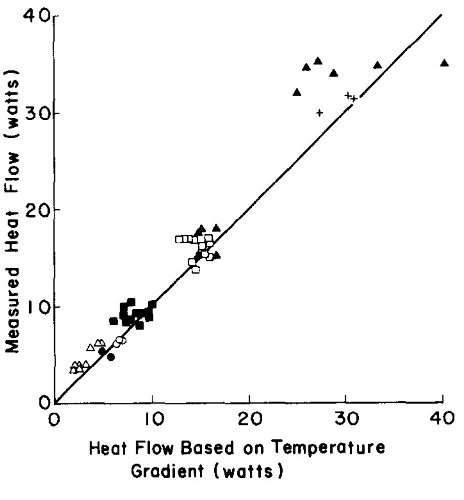

Fig. 7. Comparison of measured power input and the heat flow through the thermocline found using equation (1). Exp. 1 ○, exp. 2 ■, exp. 3 △, exp. 4 ●, exp. 5 □, exp. 6 ▲, exp. 7 +.

DISCUSSION

The results of the closed test-section experiments indicate that the hypothesis that molecular diffusion dominates transport through the central region of the thermocline is well justified. This appears to be so at least over the range of stability numbers, $5 \leqslant Sy_T \leqslant 13$, and heat fluxes, $24 \leqslant F_H \leqslant 325$ W/m^2, covered in these experiments. The data on the heat flow comparison curve, Fig. 7, fall within the accuracy of the experimental measurements.

The thickness of this diffusion dominated region increases with overall stability number. A plot of the measured diffusion thickness as a function of stability number is shown in Fig. 8 for all of our heat-salt experiments. Also shown in this figure are the thicknesses estimated from Shirtcliffe's [4] profile measurements in a transient salt–sugar experiment. While the trends are similar the stability number levels for equal thicknesses are substantially different for the two systems. To distinguish that part of the difference due to the difference in the experimental procedures one next examines the implications of these observations.

It appears that at these high stability numbers the system can be divided into three regions: a central diffusive region of thickness L through which heat and

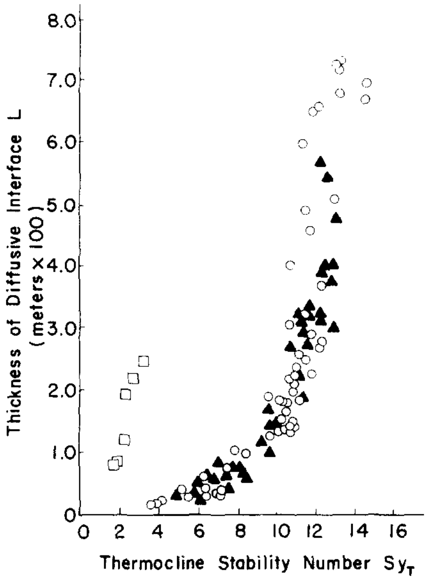

Fig. 8. Thermocline diffusion thickness vs thermocline stability number. The circles are from the permeable boundary experiment, the triangles from the closed test section experiments and the squares from Shirtcliffe's salt–sugar experiments.

salt are transported by the local gradients in temperature and concentration and two bounding convective regions where turbulent mixing takes place. Transport through the convecting regions should depend on the temperature and concentration differences across the boundary layers bordering the central diffusive layer.

With this model of the system structure the thickness of the diffusion region can be related to the heat flux and temperature and concentration differences. Assuming steady state conditions in which the vertical fluxes of heat and salt are constant and also assuming that the fluid properties are constant, one writes

$$F_H = K\frac{\Delta T_L}{L} \tag{3}$$

and

$$F_C = D_c\frac{\Delta C_L}{L} \tag{4}$$

for the diffusive region and

$$F_H = Nu_l\frac{K}{l}\Delta T_l \tag{5}$$

and

$$F_C = Sh_l\frac{D_c}{l}\Delta C_l \tag{6}$$

for the convective boundary layers. The bulk-to-bulk temperature and concentration differences may be expressed in terms of the changes in temperature and concentration across the diffusive interface and boundary layers as

$$\Delta T_T = \Delta T_L + 2\Delta T_l \tag{7}$$

and

$$\Delta C_T = \Delta C_L + 2\Delta C_l \tag{8}$$

for symmetric boundary layers. These equations can be combined along with the definition of stability number to yield

$$L = \frac{K\Delta T_T}{F_H}\left\{\frac{Sy_T/Sy_l - 1}{\dfrac{Sh_l}{Nu_l} - 1}\right\}. \tag{9}$$

The same relation obtains for assymetric boundary layers providing that the ratio Sh_t/Nu_t is the same for both.

Veronis [11] found from theoretical considerations that

$$\frac{Sh_l}{Nu_l} = \sqrt{(Le)} \tag{10}$$

for turbulent layers.

In the present experiments temperatures and concentrations in the well mixed regions of the convecting layers were accurately measured and consequently Sy_T was easily obtained. On the other hand, Sy_l which depends on the small differences in temperature and concentration across the boundary layers could not be reliably estimated by use of the profiles through the thermocline. Slight variations in the point of departure from the constant gradient region within the thermocline did not significantly alter the estimate of L but did change the value of Sy_l completely.

It is possible to determine Sy_l indirectly from the measured data since

$$Sy_l = \frac{Le}{Sh_l/Nu_l}\left[\frac{\beta_c F_C K}{\beta_t F_H D_t}\right]. \tag{11}$$

With equation (10) for the ratio of Sherwood to Nusselt number for the boundary layer this expression reduces to

$$Sy = \sqrt{(Le)}\left[\frac{\beta_c F_C K}{\beta_t F_H D_t}\right]. \tag{12}$$

Turner found in his experiments that for $Sy_T > 2$ the quantity in the brackets was essentially constant at 0.15. Using his reported value of 67 for the Lewis number in equation (12) gives 1.23 for the boundary-layer stability number. For Shirtcliffe's salt–sugar experiments the constant value of 0.6 for the flux ratio corresponds to a boundary-layer stability number of one. In the present experiments within the range $75 \leqslant Le \leqslant 110$ the flux ratio based on gradient measurements varied between 0.10 and 0.25 even when data in the transient initial period of each run and following large perturbations to the overall temperature and concentration differences are neglected. The mean value of the boundary-layer stability number calculated from these data using equation (12) is 1.58 with a standard deviation of 0.45.

Figure 9 gives a comparison between the measured diffusion length and the prediction of equation (9) based on a constant value of 1.58 for the boundary-layer stability number, square root of the Lewis number for the ratio of boundary-layer Sherwood to Nusselt numbers and the measured values of heat flux, overall temperature difference and overall stability number for each data point. The correlation over the range $4 \leqslant Sy_T \leqslant 14$

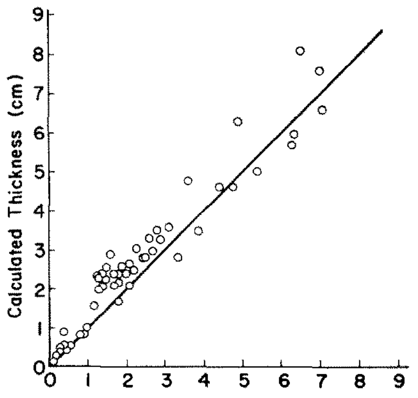

FIG. 9. Diffusion thickness measured in permeable boundary experiment compared with that calculated from equation (9) using $Sy_l = 1.58$.

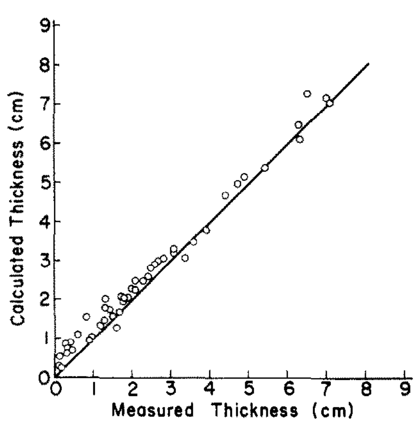

FIG. 10. Diffusion thickness measured in permeable boundary experiment compared with that calculated from equation (9) using the value of Sy_l calculated at each point.

for this data is fairly good, but much better agreement between measured and calculated values is obtained by using the measured boundary-layer stability number for each data point as shown in Fig. 10. In general, higher values for boundary-layer stability number (flux ratio) are observed at higher overall stability numbers, but the scatter in the data indicates that a simple correlation between these two variables is not appropriate. The diffusion thicknesses predicted by equation (9) for Shirtcliffe's salt–sugar system with $Sh_l/Nu_l = \sqrt{3}$ and $Sy_l = 1$ are larger than the measured values shown in Fig. 8. The discrepancy increases steadily with increasing overall stability number from about 30% at the lowest stability number to over an order of magnitude at the highest. When the fluxes based on the gradients of concentration (rather than on the change in concentration in the convecting regions) are used to define the boundary-layer stability number the agreement between the measured and calculated thicknesses generally improves but the calculated value remains consistently greater. The boundary-layer stability number based on the gradient measurements increases steadily with increasing overall stability number from 0.87 to 1.73.

Clearly, the Lewis number effect indicated by the steady-state view of the interface is sufficiently strong to account for the observed stability number dependence of the diffusion thickness shown in Fig. 8. Quantitative differences between the thicknesses observed and predicted on the basis of the steady state model may be due to the transient nature of the experiments, particularly the salt–sugar experiments.

The upward migration of the interface noted in all of our experiments indicates some assymetry in the system, although equation (9) holds for assymetric boundary layers as long as Sh_l/Nu_l is the same for both boundary layers. Several experiments were run in the closed test section apparatus with the temperature of one of the convecting layers deliberately mismatches with the temperature of the surrounding wall to see if convection currents associated with sidewall heat transfer in either the upper or lower layer might be responsible for the observed rise. No change in direction of migration and no apparent change in rate could be observed during these runs.

CONCLUSIONS

Two quasi-steady experiments in layered thermohaline convection show that the interface between two well-mixed convecting layers broadens as the overall stability number $\beta_c \Delta C_T / \beta_t \Delta T_T$ increases. These experiments further indicate that heat and salt transport through the central region of the interface is by molecular diffusion. These results are in qualitative agreement with Shirtcliffe's [4] findings for a salt–sugar system. For comparable interface thicknesses, however, much higher values of stability number are observed in the heat–salt experiments.

A model of the interface at high stability numbers based on observations consists of a central quiescent diffusion region surrounded by two convecting boundary layers. The observations interpreted on the basis of the steady-state implications of this model suggest that the thickness of the diffusive layer adjusts to maintain conditions of near neutral stability across the boundary layer, $Sy_l = 1$.

Sufficiently significant deviations from neutral boundary-layer stability are obtained, however, to indicate that this parameter is not constant in interfacial boundary layers.

REFERENCES

1. J. S. Turner, *Buoyancy Effects in Fluids*. Cambridge University Press, Cambridge (1973).
2. J. S. Turner, Double-diffusive phenomena, in *Annual Review of Fluid Mechanics*, edited by M. Van Dyke, W. G. Vincenti and J. V. Wehausen, Vol. 7, pp. 37–56. Annual Reviews, Palo Alto (1974).
3. J. S. Turner, The coupled turbulent transports of salt and heat across a sharp density interface, *Int. J. Heat Mass Transfer* **8**, 759–767 (1965).
4. T. G. L. Shirtcliffe, Transport and profile measurements of the diffusive interface in double-diffusive convection with similar diffusivities, *J. Fluid Mech.* **57**, 27–43 (1973).
5. P. F. Linden, A note on the transport across a diffusive interface, *Deep-Sea Res.* **21**, 283–287 (1974).
6. H. E. Huppert, On the stability of a series of double-diffusive layers, *Deep-Sea Res.* **18**, 1005–1021 (1971).

7. J. M. Broughton, Experiments on steady layered convection in a doubly diffusive system, M.S. Thesis, Colorado State University (1972).
8. D. E. Lamb, F. S. Manning and R. H. Wilhelm, Measurements of concentration fluctuations with an electrical conductivity probe, *A.I.Ch.E. Jl* **6**, 682–685 (1960).
9. W. D. Clements, Jr. and C. B. Schnelle, Jr., Electrical conductivity in dynamic testing, *ISA Jl* **10**, 63–68 (1963).
10. T. R. Mancini, Layered thermohaline natural convection, Ph.D. Thesis, Colorado State University (1975).
11. G. Veronis, On finite amplitude instability in thermohaline convection, *J. Mar. Res.* **23**, 1–17 (1965).

CONVECTION NATURELLE DES SOLUTIONS THERMOSALINES STRATIFIEES

Résumé—Les résultats de deux expériences quasi-stationnaires de convection double en présence de diffusion dans un fluide stratifié sont présentés et interprétés à l'aide d'un modèle stationnaire. Dans les expériences, la chaleur et le sel s'élèvent, transportés au travers de deux couches de convection horizontales d'eau séparées par une thermocline, région à gradients de température et de concentration élevés. Lorsque le nombre $\beta_C \Delta C/\beta_t \Delta T$ caractéristique de la stabilité de la thermocline s'accroit, la thermocline s'épaissit et les flux de chaleur et de sel diminuent. On montre que ces deux caractères du système thermosalin sont compatibles avec un modèle de conduction et de convection qui considère la thermocline comme une région de conduction séparant deux couches limites de convection. On vérifie par voie expérimentale le fait que la diffusion moléculaire est le processus de transport dominant dans la région centrale de la thermocline. On a trouvé que l'épaisseur de la région de conduction varie avec les conditions aux limites imposées de telle manière que les conditions approchées de stabilité neutre soient maintenues à travers les couches limites.

NATÜRLICHE KONVEKTION IN EINEM GESCHICHTETEN THERMOHALINEN SYSTEM

Zusammenfassung—Die Ergebnisse von quasi-stationären Versuchen bei geschichteter doppeldiffuser Konvektion werden wiedergegeben und interpretiert in Form eines stationären Modells. In den Versuchen wurde Wärme und Salz nach oben transportiert durch zwei waagerechte Konvektionsschichten aus Wasser, die durch eine Thermokline getrennt waren einem Bereich großer Temperatur- und Konzentrationsgradienten. Mit Zunahme der für die Stabilität der Thermoklinen charakteristischen Zahl $\beta_c \Delta C/\beta_t \Delta T$ wird die Thermokline dicker, und der Wärmefluß und der Transport von Salz nimmt ab. Diese beiden Charakteristika des thermohalinen Systems erweisen sich als konsistent mit einem Leitungs-Konvektions-Modell, das die Thermokline als einen Leitungsbereich darstellt, der zwei konvektive Grenzschichten trennt. Es ist experimentell nachgewiesen, daß die molekulare Diffusion den dominierenden Transportprozeß im Mittelbereich der Thermoklinen darstellt. Die Dicke der leitenden Schicht ist veränderlich mit den aufgeprägten Randbedingungen in der Weise, daß die Voraussetzungen einer nahezu neutralen Stabilität über die Grenzschichten hinweg erhalten bleibt.

СЛОИСТАЯ ТЕРМОГАЛИННАЯ ЕСТЕСТВЕННАЯ КОНВЕКЦИЯ

Аннотация — Представлены результаты двух квазистационарных экспериментов по слоистой конвекции бинарной смеси, которые анализируются на основе стационарной модели. В экспериментах тепло и соль переносились конвекцией вверх через два горизонтальных слоя воды, разделенных термоклином — областью больших температурных и концентрационных градиентов. По мере того, как критерий устойчивости термоклина $\beta_C \Delta C/\beta_t \Delta T$ возрастает, термоклин становится толще, и потоки тепла и соли уменьшаются. Показано, что эти две характеристики термогалинной системы согласуются с кондуктивно-конвективной моделью, которая рассматривает термоклин, как область теплопроводности, разделяющую два конвективных пограничных слоя. Экспериментально подтверждается, что в центральной части термоклина преобладает перенос за счёт молекулярной диффузии. Найдено, что толщина области теплопроводности изменяется с изменением граничных условий таким образом, чтобы в пограничных слоях сохранить условия, близкие к нейтральной устойчивости.